Ab initio density functional investigation of B_{24} clusters: Rings, tubes, planes, and cages

S. Chacko* and D. G. Kanhere[†]

Department of Physics, University of Pune, Pune 411 007, India

I. Boustani[‡]

Universität Wuppertal, FB 9 - Theoretische Chemie, Gauß Straße 20, D-42097 Wuppertal, Germany

We investigate the equilibrium geometries and the systematics of bonding in various isomers of a 24-atom boron cluster using Born-Oppenheimer molecular dynamics within the framework of density functional theory. The isomers studied are the rings, convex and quasiplanar structures, the tubes, and closed structures. A staggered double ring is found to be the most stable structure among the isomers studied. Our calculations reveal that a 24-atom boron cluster does form closed three-dimensional structures. All isomers show a staggered arrangement of nearest-neighbor atoms. Such a staggering facilitates sp^2 hybridization in boron clusters. A polarization of bonds between the peripheral atoms in the ring and planar isomers is also seen. Finally, we discuss the fusion of two boron icosahedra. We find that the fusion occurs when the distance between the two icosahedra is less than a critical distance of about 6.5 a.u.

I. INTRODUCTION

Atomic clusters are of great interest due to their novel properties which can serve as building blocks for self-assembled material in order to realize miniaturized nanodevices. Due to the increasing technological importance of nanoscale devices, the investigation of the structural and the related physical and chemical properties of clusters, especially boron, carbon, and silicon-based systems, is becoming an expanding research area.

The discovery of the C_{60} carbon buckminsterfullerene molecule[1] and its unique electronic properties has triggered an explosive growth of research in the field of cluster physics. Superconducting and magnetic fullerides,[2] atoms trapped inside the fullerene cage, chemically bonded fullerene complexes have generated much excitement. Since then, much attention has been focused on fabricating small caged clusters of various elements like C, Si, and B. However, small clusters of silicon and carbon ($n<15$) do not form stable cage structures. One of the ways of stabilizing these cages is by trapping a foreign atom at the center of the cage. Recent work by Kumar and Kawazoe demonstrated the feasibility of metal encapsulation of fullerene-like caged clusters of Si.[4]

On similar grounds it would be interesting to look at boron cages, since boron and boron-rich compounds exhibit some of the most interesting chemistry of all elements in the periodic table.[5] Atomic boron is the first light element of group III with one p valence electron.[3] It is semiconducting in its bulk phase with low density, a very high melting point, and hardness close to that of diamond. Due to sp^2 hybridization of the valence electron, large coordination number, and short covalent radius, boron prefers to form strong directional bonds with various elements.

Boron clusters have been investigated mainly via computer simulations although some experimental results are available. La Placa *et al* proposed the existence of $B_{36}N_{24}$ clusters with the same structure as that of the fullerene C_{60}.[6] However, the only heteroatomic species that were observed

in the experiment were BN and B_2N. In contrast, an earlier experiment had detected the existence of $B_nN_m^+$ for various combinations of n and m for $n=2-17$ (Ref. 7). Other abundant distribution and fragments of clusters of group III were also found.[8] Niu, Rao, and Jena carried out a comprehensive theoretical study of the equilibrium geometries, vertical ionization potentials, and the fragmentation patterns of B_2-B_6 clusters in neutral and singly charged states, as well as the stability of boron-rich clusters, B_nX, $n=1,5,12$, $X=$ Be,C (Ref. 9). They show that the electronic bonding in boron clusters is similar to that in boron-rich solids and is characterized by a three-center bond. In spite of being a trivalent element having three centered bonds, a B_{20} dodecahedron composed of pentagonal faces with each atom being threefold coordinated does not exhibit the unusual stability.[9] *Ab initio* investigations of small boron clusters by Boustani reveal that most of the stable structures are composed of two fundamental units: hexagonal or pentagonal pyramids.[10] Hayami has investigated the encapsulation of impurity atoms, from H to Ne, in B_{12} (Ref. 11) icosahedron. He found that H and Li are most likely to get trapped and stabilize the cage. He also found that the highest occupied molecular orbital (HOMO) and lowest unoccupied molecular orbital (LUMO) gap is largest for C.

Boron exists in various crystalline and amorphous forms of which α-, β-rhombohedral (α-rh and β-rh) and α- tetragonal (α-tet) are well-known phases.[5] The α- and β-rh boron solids are composed of unit cells containing B_{12} icosahedra. The α-rh boron, also called low-temperature or red boron, has a high level of crystal purity. The B_{12} icosahedra in this form are slightly distorted which are weakly bound to each other by three-center bonds situated in alternating parallel planes. This leads to weak thermal stability, and therefore α-rh boron on annealing at a temperature of about 1200 °C transforms into β-rh. In contrast, a hypothetical α-rh boron quasicrystal contains two elemental unit cells: a prolate and an oblate, stacked in a quasiperiodic manner.[12,13] The prolate

unit cell in the quasicrystal is slightly distorted which transforms into an oblate unit cell to form the quasicrystal. The formation of such an icosahedral quasicrystal is also seen in Al-Mn alloy.[14] An interesting question concerns the transformation of the distorted prolate unit cells into an oblate unit cell. Takeda *et al.* found that the mechanism of this transition as an interpenetrating process of the two B_{12} icosahedra lying along the short body diagonal in a prolate cell in the quasicrystal.[15] Boustani and co-workers investigated the fusion of those two B_{12} icosahedra lying along the short body diagonal.[16] Their calculations reveal that a stable drumlike boron cluster can be formed without removing any atoms within the two approaching icosahedra as suggested by Takeda *et al.* They have considered various configurations of two B_{12} icosahedra connected to each other in different orientation. The optimization and search for local minima was performed with certain symmetry restrictions. The relative stability of these geometries were not compared with the other possible isomers of the 24-atom boron cluster. This is especially important since the geometrically most stable isomer of B_{24} could be completely different from the drumlike structure and could be much lower in energy.

In the present work, we address some of these questions concerning the fusion of two boron icosahedra and the B_{24} cluster. It is known that the number of isomers on an energy surfaces increases exponentially with the size of the cluster. Since B_{24} is a medium-size cluster, it has a large number of isomers. An interesting aspect of medium-size boron clusters is the competition between quasiplanar, tubular, and closed structures.[17] The strains in the bonds due to the curvature in closed structures favor quasiplanar structure, whereas the dangling bonds in quasiplanar and convex structures favor tube and cage isomers. We discuss the energetics, stability, and bonding properties in certain representative isomers of the 24-atom boron cluster, followed by a discussion of the process of fusion of two B_{12} icosahedra. Previous reports as well as our investigation reveals that such a fusion results in a closed structure. Although this structure is stable, it need not be the lowest-energy isomer. In order to understand the relative stability of this fused structure and, hence, the stability of the quasicrystal, we have investigated the various representative low-lying structures of the 24-atom boron cluster.

In Sec. II, we describe the numerical method used followed by a discussion of the results in Sec. III.

II. THEORETICAL DETAILS

We employ Born-Oppenheimer molecular dynamics (BOMD) based on *Kohn-Sham* (KS) formulation of density functional theory using the damped equation[18] method within the pseudopotential approximation.

The electronic structure and total energy of the isomers have been computed using ultrasoft pseudopotentials[19] within the local density approximation (LDA) and the generalized gradient approximation (GGA) using the VASP (Ref. 26) package. The Ceperley-Alder[20] exchange-correlation potential for the LDA and Perdew-Wang[21] potential for the

TABLE I. Size of the supercell (in Å) for various isomers.

Isomer	Simulation cell (Å)
Ring 1×24	$18 \times 18 \times 4$
Ring 1×24	$17 \times 17 \times 11$
Tube 3×8	$14 \times 14 \times 13$
Tube 4×6	$15 \times 15 \times 16$
Quasiplanar and Convex	$15 \times 15 \times 10$
Cages	$13 \times 13 \times 15$

GGA have been used. The geometries were optimized using the conjugate gradient and the steepest descent method.[18] The size of the simulation cell was varied according to the structure studied. (See Table I).

The structures were considered to be converged when the force on each ion was less than 0.01eV/Å with a convergence in the total energy of about 10^{-4}–10^{-6}eV.

The fusion of two icosahedra was carried out using the inhouse package. The norm-conserving pseudopotential of Bachelet *et al.*[22] in Kleinman- Bylander[23] form with *s* part treated as nonlocal was employed. The exchange-correlation potential by Ceperley and Alder[20] was used. A cubic supercell of length 40 a.u. with an energy cutoff of 21.0 Ry provided sufficient convergence in the total energy. During the dynamics, the norm of each of the states, defined as $|h\psi_i - \epsilon_i\psi_i|^2$ (ϵ_i being the KS eigenvalue corresponding to the KS eigenstate ψ_i), was maintained at 10^{-7}–10^{-9} a.u. The final structures were considered to be converged when the forces on all atoms were less than 10^{-4} to 10^{-3} a.u.

The nature of the bonding has been investigated using the electron localization function[24] (ELF) along with the charge density. Such ELF[24] have been found to been useful for elucidating the bonding characteristics of a variety of systems, especially in conjunction with the charge density. For a single determinantal wave function built from KS orbitals ψ_i, the ELF is defined as

$$\chi_{ELF} = \left[1 + \left(\frac{D}{D_h} \right) \right]^{-1},$$

where

$$D = \frac{1}{2} \sum_i |\nabla \phi_i|^2 - \frac{1}{8} \frac{|\nabla \rho|^2}{\rho},$$

$$D_h = \frac{3}{10} (3\pi^2)^{5/3} \rho^{5/3},$$

with $\rho = \rho(\mathbf{r})$ the valence-electron density. A value of χ_{ELF} of nearly 1 represents a perfect localization of the valence electron density.[24]

III. RESULTS AND DISCUSSION

The present investigation can be separated into two groups. First, we present results for various isomers of a 24-atom boron cluster which can be classified into the, (i)
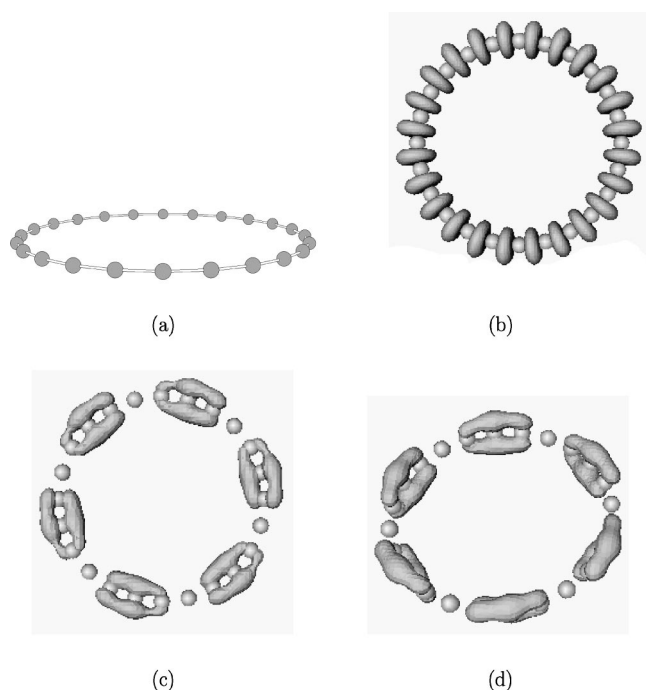
FIG. 1. (a) The optimized geometry of the monocyclic ring of 24 boron atoms. (b) The isovalued surface of the ELF at the value 0.75. (c) The isovalued charge density surface of the HOMO state at the value 0.0059 electron/Å³. (d) The isovalued charge density surface of the LUMO state at the value 0.0052 electron/Å³.
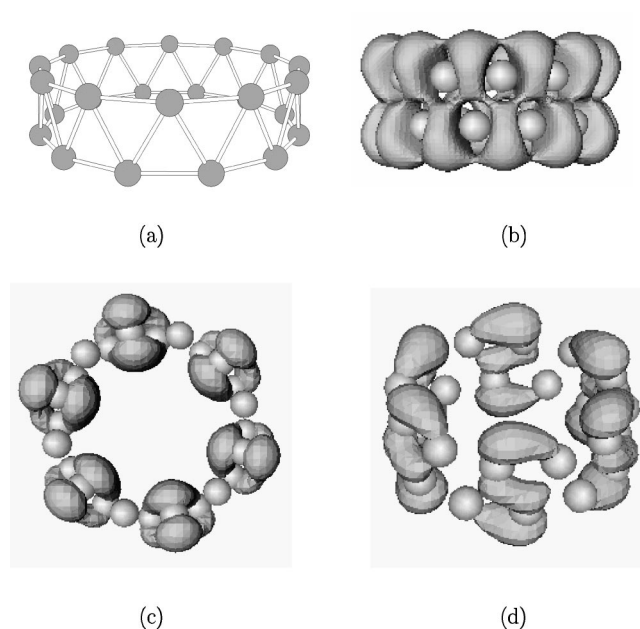

FIG. 2. (a) The optimized geometry of the double ring of 24 boron atoms. (b) The isovalued surface of the ELF at the value 0.75. (c) The isovalued charge density surface of the HOMO state of the double ring at the value 0.0075 electron/Å³. (d) The isovalued charge density surface of the LUMO state of the double-ring at the value 0.0091 electron/Å³.

rings, (ii) tubes, (iii) convex and quasiplanar structures, and (iv) closed structure isomers of B_{24}. Since B_{24} has a large number of isomers, we restrict our study to certain isomers of the above representative classes. First, we discuss the geometry and bonding in these isomers computed by the GGA, followed by the energetics and stability of these isomers. Finally, we discuss the fusion of two boron icosahedra.

A. Isomers of B_{24}

1. Rings

In this section, we present the results for two rings: viz., a monocyclic ring and a double ring. In Fig. 1, we show the optimized geometry, the isovalued surfaces of the electron localization function, and the total charge density for the HOMO and LUMO states for the monocyclic ring. It turns out that this structure is the least stable and makes an interesting contrast with the most stable structure: viz., the double ring.

The monocyclic ring has a diameter of 11.81 Å. In spite of being the least stable isomer, the ELF plot, in Fig. 1(b), shows a localized p_x-$p_x \sigma$ bond. It is interesting to examine the behavior of the HOMO state. The HOMO state in the monocyclic ring is doubly degenerate. In Fig. 1(c), we show the charge density for the one of the HOMO state. It can be noted that the π bond has six spatial nodes. The other HOMO state is similar to this state with a phase shift. As a result, an effective delocalization of the π bonds similar to that in benzene[25] is seen. The difference in the HOMO states

of benzene and B_{24} are that in benzene the π bonds are perpendicular to the plane of the carbon ring, whereas in B_{24} the HOMO is formed by the in-plane p_y-p_y orbitals. During the formation of the benzene molecule, each carbon atom promotes an electron from the $2s^2$ state into the empty $2p_z$ orbital, whereas in boron an electron from the $2s^2$ state is promoted to the empty $2p_y$ orbital. Thus, the reason for formation of in-plane π bonds in B_{24} is the absence of p_z electrons. The LUMO state of B_{24}, on the other hand, is out of the ring plane p_z-p_z [Fig. 1(d)].

In Fig. 2 we show the optimized geometry, the isovalued surfaces of the electron localization function, and the total charge density for the HOMO and LUMO states for a double ring. The double ring of diameter 6.22 Å is composed of two rings of 12 atoms each, 1.45 Å apart, arranged in a staggered configuration. Each ring is rotated by an angle of $\pi/12$ with respect to the other ring in order to form the staggered configuration. It is known that boron, boron-rich compounds, and boron clusters exhibit sp^2 hybridization. Such a staggered double-ring formation facilitates such a hybridization, thereby making it the most stable structure.

The ELF plot [Fig. 2(b)] shows a polarized σ bond between the atoms in the same ring, the polarization caused by the atoms in the neighboring ring. This is a signature of a three-centered boron bond which is a precursor to the bonding in solid-state boron. The total charge density (not shown) is also localized in the region between the two rings. The charge density for the HOMO [Fig. 2(c)] and the LUMO [Fig. 2(d)] represents a strongly localized π bond between two atoms. While the HOMO state is a π bond between an atom of each ring, the LUMO state shows a lateral p-p over-
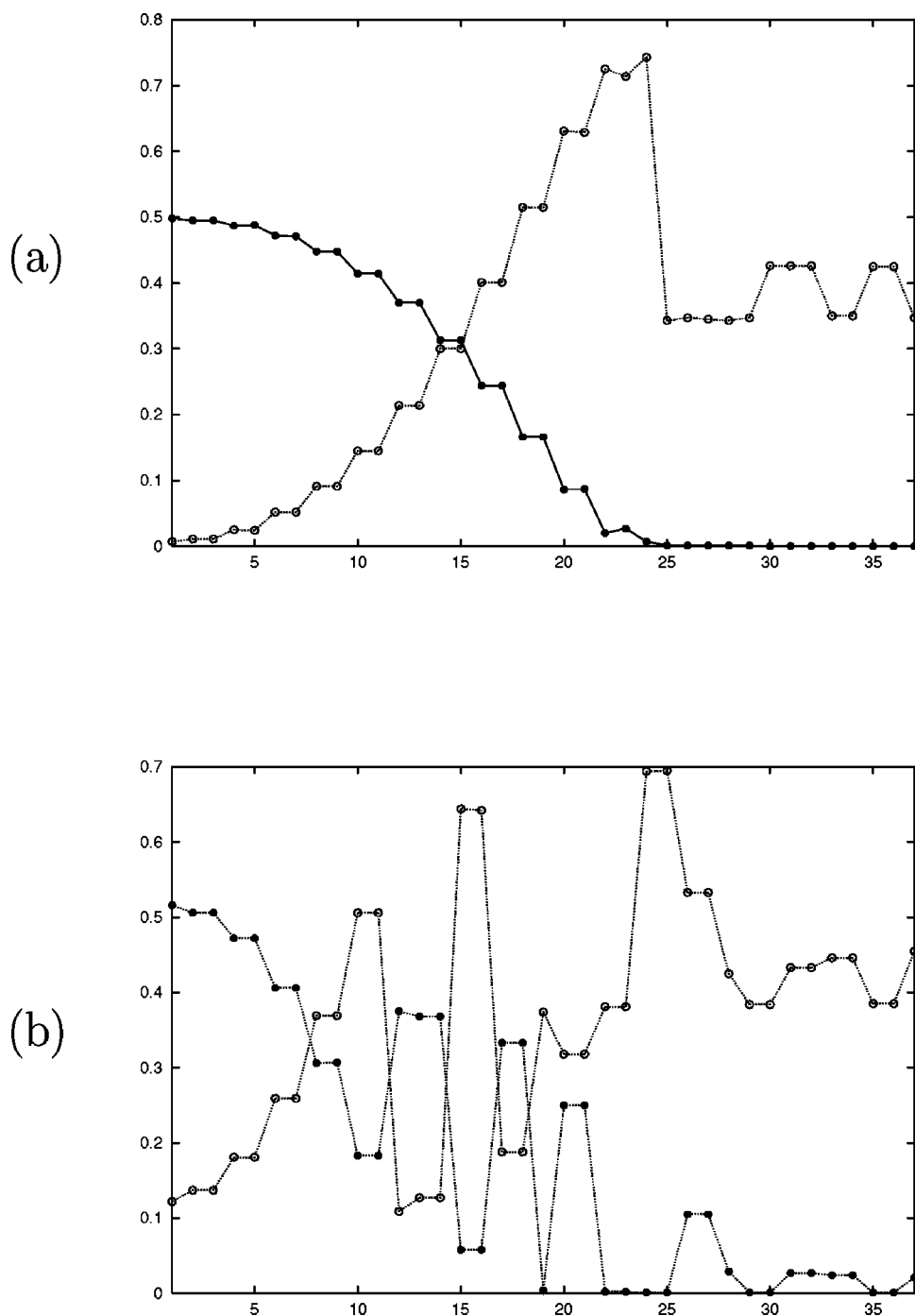
FIG. 3. The amount of s (solid line) and p character (dotted line), in arbitrary units, in various occupied states and the LUMO state as a function of orbital number for (a) the monocyclic ring and (b) the double ring.

lap between the atoms of both rings. Similar to the monocyclic ring, the HOMO state in this case is also doubly degenerate, giving rise to an effective delocalization.

It is instructive to analyze the total p character in the orbitals as a function of orbital number. In Figs. 3(a) and 3(b), we show such a plot for monocyclic and double rings, respectively. The character in the orbitals is calculated by projecting the orbitals onto spherical harmonics centered at each ionic sites within a sphere of a specified radius around each ion. The radius of the sphere is usually taken to be half of the distance of the ion from the nearest ion. It can be noted that a monotonic decrease in the amount of s character in a monocyclic ring is seen, whereas it is oscillatory for the double ring in the centrally occupied orbitals. A substantial amount of p character in the lower occupied states in the double ring is seen. This indicates a higher degree of sp hybridization. For both structures, a double degeneracy is seen in most of the occupied states. These states represent resonant structures.

2. Tubes

We discuss three tubes composed of (a) three planar rings of eight atoms, (b) four planar rings of six atoms, and (c) four rings, each ring consisting of six atoms arranged in a staggered configuration.
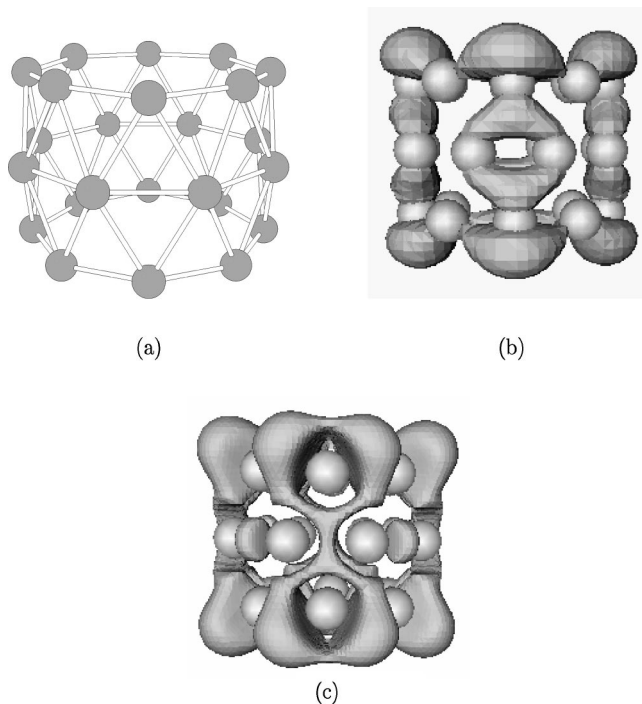
(a)   (b)

(c)

FIG. 4. (a) The optimized geometry of the drum-shaped B_{24} cluster composed of three rings of eight boron atoms each. (b) The isovalued charge density surface of the HOMO state at the value 0.0036 electron/$Å^3$. (c) The isovalued surface of the ELF at the value 0.75.

In Fig. 4, we show the optimized geometry of the tubular drum-shaped boron cluster along with the HOMO state and the ELF. This structure is composed of three rings of eight boron atoms each, with the height of the drum alternating between 2.92 and 3.01 Å. The surface of the drum is made up of an elongated rhombus with the atoms in the central rings coming closer to each other, thereby pushing apart the atoms on the outer rings. This structure has a distorted D_{4h} symmetry. Energetically, this structure is nearly degenerate to the double ring. It has a very small HOMO-LUMO gap (0.3 eV as compared to 1.28 eV in the double ring), due to Jahn-Teller distortions. The HOMO state is doubly degenerate, which on distortion gives rise to this small gap. The isovalued plot of the HOMO [Fig. 4(b)] shows a bond between an atom of the outermost rings with the two nearest atoms in the central ring along the bonding region, unlike the ring isomers where a π bond is formed. The peculiar alternating height is due to the characteristic bonding in this structure. The ELF [Fig. 4(c)] shows a strong localized bond between the central atoms of the rhombus. The bonds among the outer-ring atoms are similar to that of the double ring— i.e., polarized by the atoms in the central ring.

A four-ring tube with six boron atoms each is shown in Fig. 5(a). This tube with a small diameter of about 3.0 Å is the initial structure. On geometry optimization, the open tubular structure distorts, thereby closing both ends. The optimized geometry is shown in Fig. 5(b). It is seen that alternate atoms in the outermost rings on either side approach the center of the ring closing the ends. This structure can also be

viewed as a distorted cage, as shown in Fig. 7(b), below, without the icosahedral closing. It is interesting to note that, despite sp^2 hybridization, there is a possibility of getting a three-dimensional (3D)closed structure.

We have also carried out a geometry optimization of a B_{24}-D_{3d} open structure. The geometry of this structure is depicted in Fig. 5(c). This structure too undergoes a similar structural transformation into a closed D_{3d} boron cage [Fig. 7(b) below], due to higher bond strains and a large curvature at the open ends. This result is contradictory to that reported by Boustani and co-workers.[16] According to them, the stability of the closed tubular form B_{24}-D_{3d} increases when the closed tubular ends rearrange to form an additional ring of six atoms, as found within an open tubular structure of B_{24}-D_{6d}. This difference is mainly due to the differences in the theoretical approaches. We have done unrestricted geometry optimization, whereas they have imposed a certain symmetry restriction for the minimization. Moreover, we have used the density functional method within plane-wave pseudopotential and GGA approximations, whereas Boustani *et al.* have done all-electron calculations using Hartree-Fock and local spin density functional theory.

3. Quasiplanar and convex structures

We present the results for a couple of open structures: viz, the quasiplanar and the convex stable isomers of B_{24}. According to the *Aufbau principle* proposed by Boustani,[10] we construct a quasiplanar and a convex structure from the basic unit of a hexagonal pyramid B_7. Upon optimization, we find that the LDA-computed geometry of the quasiplanar structure is nearly planar. The quasiplanarity comes from the GGA calculations. The GGA-optimized geometry of the quasiplanar structure is shown in Fig. 6(a). Some atoms are raised above the plane while some atoms are shifted below the plane, leading to a staggered configuration. Thus, even the open structures, staggering is preferred. The convex structure, on the other hand, gets distorted by the both LDA as well as the GGA, although the convexity is maintained. This distorted structure is depicted in Fig. 6(d). It can be noted that both these isomers—the quasiplanar and convex— have nearly similar structure. However, the HOMO state of these structures differ drastically. In Fig. 6(b), we show the isovalued plot of the HOMO state of the quasiplanar structure at 1/10th of its maximum value. The HOMO state is delocalized within the plane along the bonding region. An excess electron cloud outside the cluster is also seen. This behavior in the HOMO state of the quasiplanar structure can be contrasted with that of the convex structure. In Fig. 6(e), we show the plot of the HOMO state for the convex structure at 1/6th of the maximum value. It is clear from this plot that the HOMO state is more localized. It represents a π bond between atoms of the outermost layer, the π bond being formed on the two sides of the plane of the structure.

In Figs. 6(c) and 6(f), we plot the ELF for these two structures, respectively. The nature of the ELF in both structures is nearly similar. A polarization of the bond between the peripheral atoms is seen in both cases. A higher degree of polarization in the quasiplanar structure is seen. Moreover, a
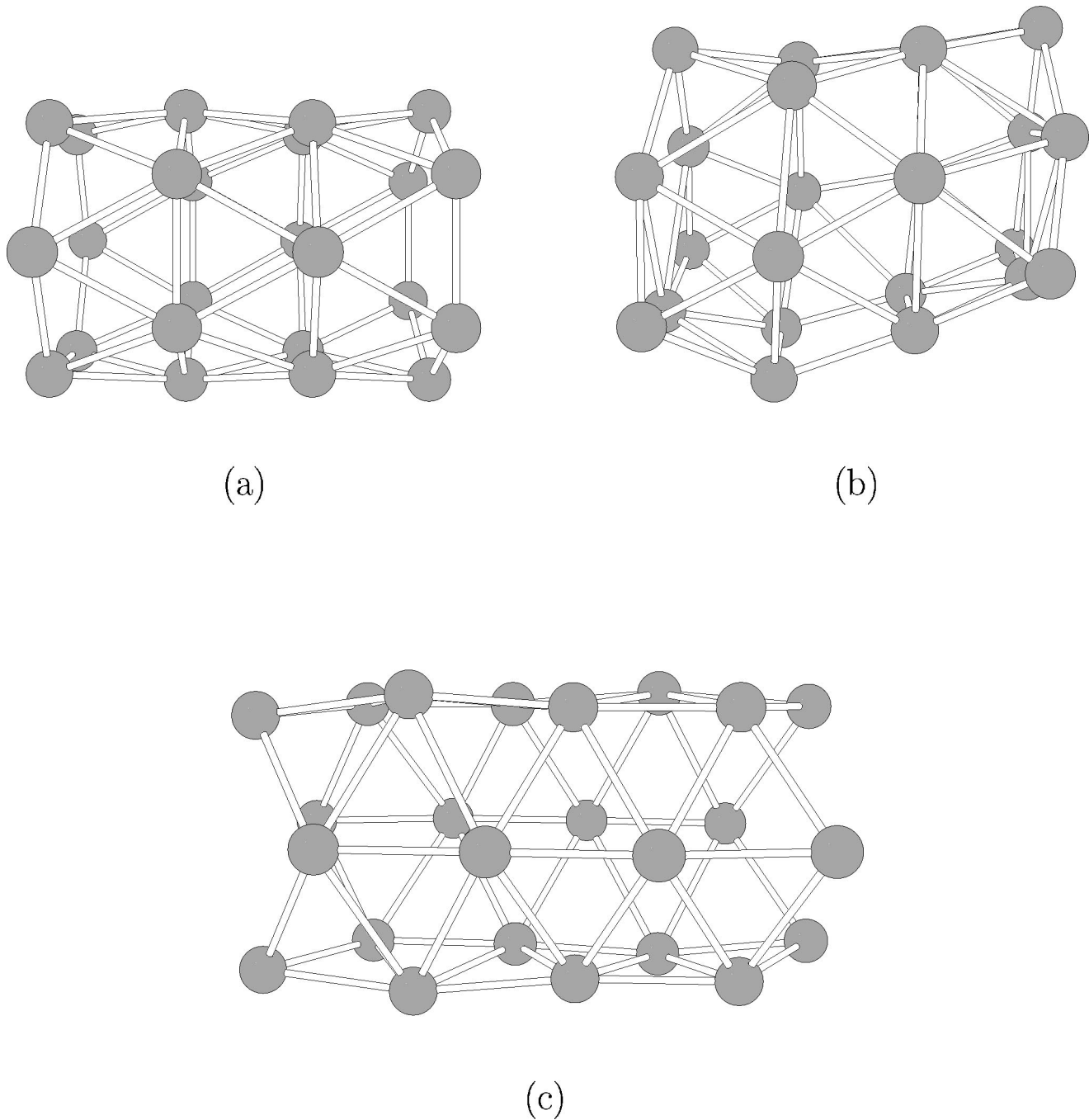
FIG. 5. (a) The initial geometry of the four-ring tube, each ring formed by six boron atoms. (b) The optimized structure. (c) The open tube with D_{3d} symmetry composed of four rings of staggered B_6.

three-centered bond is seen in interior atoms in the quasiplanar structure.

4. Closed Structures

In this class we have studied three structures. The geometry of these structures are shown in Figs. 7[a(i)], 7[b(i)], and Fig. 7[c(i)]. We will refer these closed structures as cage I, cage II, and cage III, respectively. It is seen that upon formation of closed structure the stability of the boron isomers decreases as compared to that of the most stable isomer.

Cage I (7[a(i)]) represents two interacting B_{12}. It has D_{3h} symmetry. These two icosahedra, on fusion, transform into a closed tubular form—viz., cage II—shown in Fig. 7[b(i)]. The fusion process will be discussed later. This structure has symmetry D_{3d}. In case of cage II, it is seen that the atoms move towards the fusion region, thereby decreasing the bond strains in the icosahedral units. This structure is the most stable cage isomer of B_{24}. Cage III shows a different behavior than the other two structures. The first two cages show an icosahedral unit, whereas cage III can be visualized as a
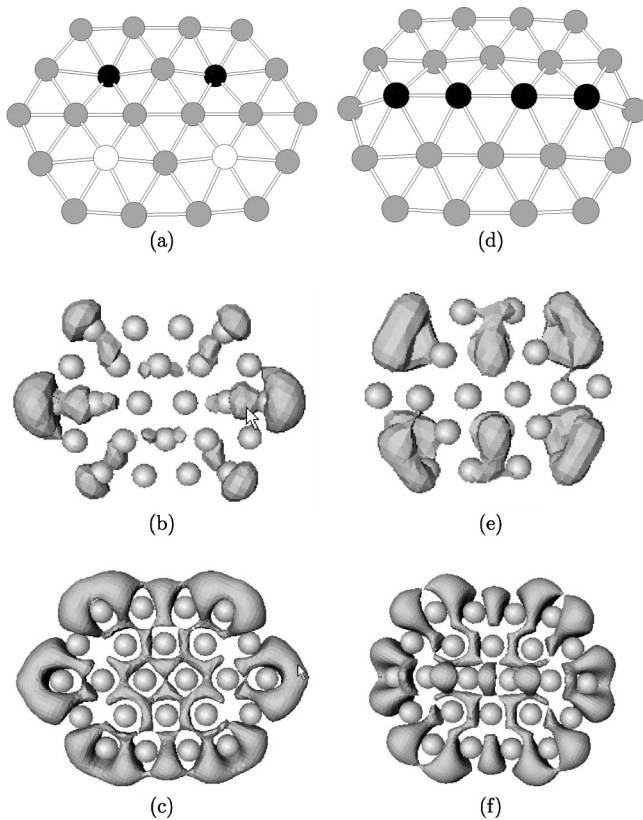
FIG. 6. (a) The optimized geometry of the quasiplanar structure. The black circles represents atoms below the plane while the white circles represents atoms above the plane, giving the quasiplanar nature. (b) The isovalued charge density surface of the HOMO state of the quasiplanar structure at the value 0.0017 electron/Å^3. This value is 1/10th of the maximum. (c) The isovalued surface of the ELF at the value 0.75. (d) The optimized geometry of the convex structure. The black circles represents atoms above the plane giving the convex nature. Remaining atoms are nearly planar. (e) The isovalued charge density surface of the HOMO state of the convex structure at the value 0.0031 electron/Å^3. This value is 1/6th of the maximum. (f) The isovalued surface of the ELF at the value 0.75.
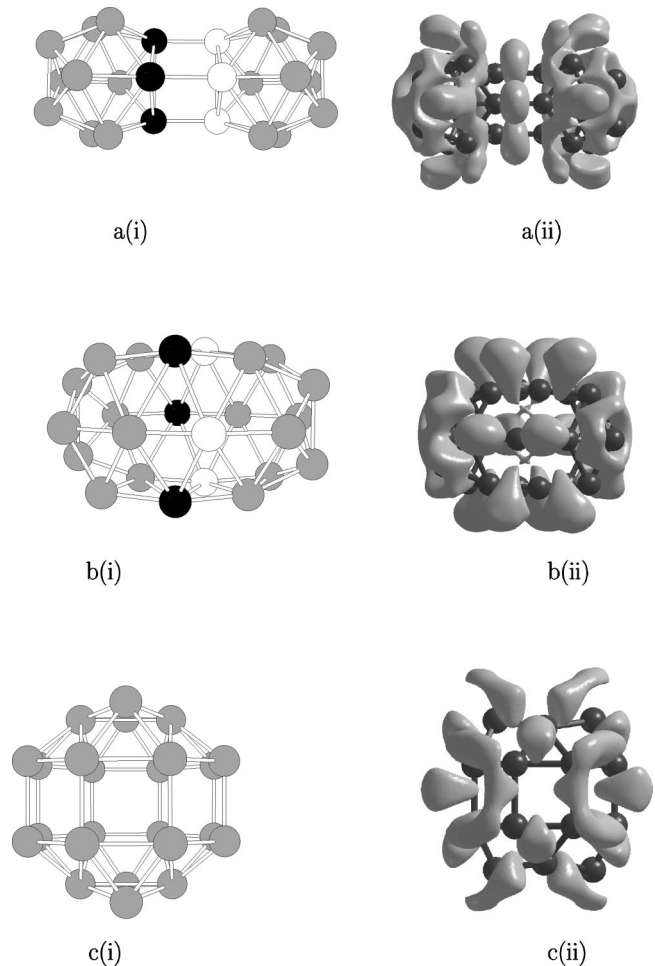

FIG. 7. The geometries of closed structures: [a(i)] cage I representing two icosahedra interacting by three bonds, each bond formed by atoms represented by black and white dots. [a(ii)] ELF plots for cage I at the value 0.75. [b(i)] cage II, the resultant structure of the fusion of two B_{12} icosahedra. A staggered-ring of six atoms (three white and three black) is seen. [b(ii)] ELF plots for cage II at the value 0.75. [c(i)] cage III, composed of two rings of eight atoms each placed side by side, and capped by four atoms on both sides. The four atoms forms a quinted-roof-like structure. [c(ii)] ELF plots for cage III at the value 0.75.

double ring of eight atoms, placed side by side. Each side of this ring is capped by four atoms which form a quinted roof or bent-rhombus-like structure. This cage turns out to be the least stable closed isomer of B_{24}.

The bonding in cages I and II is similar to that of the B_{12} icosahedra except at the fusion region. In Figs. 7[a(ii)], 7[b(ii)], and 7[c(ii)], we plot the ELF for cages I–III. It can be seen that in case of cages I and II, the ELF shows a high localization of the charge in the fusion region of the two icosahedra. A slight delocalization at the ends of the tube, as compared to the central fusion region, is seen. This shows an affinity of the boron icosahedra to get bonded to each other. On the other hand, the ELF for the cage III, depicted in Fig. 7(c), shows a three-centered bond between an atom of the quinted roof and two atoms from the octagonal ring. It is interesting to note that such bonding is seen in solid-state boron.[5] Thus, in spite of a three-centered bond, the boron clusters does not show enhanced stability.

5. Energetics and stability

The energetics and stability of isomers of B_{24} can be explained via the binding energy, content of the *p* character in the total density, and HOMO-LUMO gap. In Fig. 8(a), we plot the binding energy per atom for all isomers studied, computed by the LDA and GGA. The binding energy is calculated as $E_b = E_{atom} - E_{B_{24}}/24$. The trend in the binding energy by both methods is remarkably similar. The GGA gives lower binding energy for all isomers, the shift being nearly identical. The double ring is the most stable isomer. With the exception of the monocyclic ring and cage III, all the isomers are nearly degenerate while the double ring. The stability of the isomers can be associated with the amount of *p* character in the total charge density. In Fig. 8(c), we plot the content of
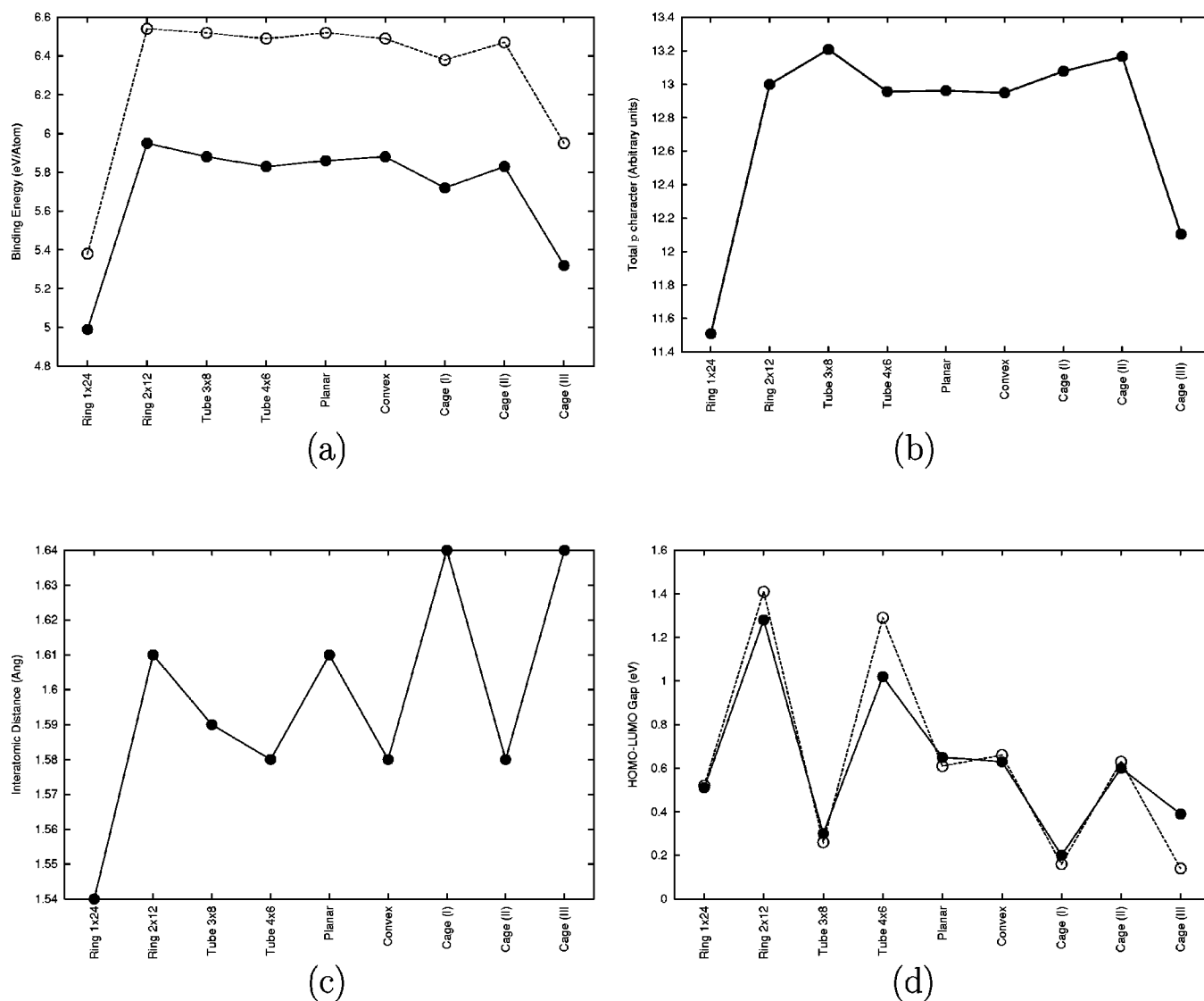
FIG. 8. (a) Binding energy in eV per atom of the various B_{24} isomer computed by the LDA and GGA. The dotted line represents the LDA binding energy while the solid line represents the GGA binding energy. (b) The amount of p character in the total density for various isomers computed by the GGA. (c) The minimum interatomic distances in various isomers computed by the GGA. (d) HOMO-LUMO gap, in eV, of the various B_{24} isomers computed by the LDA and GGA. The dotted line represents the LDA gap while the solid line represents the GGA gap.

p character in the total charge density computed by the GGA. The p character is calculated by the method discussed above. The amount of p-character in the total charge density is the sum of all projections over all ionic sites. Interestingly, the p character plot nearly follows a similar trend to the binding energy. The least stable structure—viz, the monocyclic ring—has the least p-character in the total charge density. Thus, the binding energy is largely influenced by the amount of p character contained in the total charge density. It can be noted that due to similar structure, the convex and quasiplanar structures have nearly same binding energy and the amount of p character in the total density. The lower binding energy of the monocyclic ring is not only a result of a lower content of p character but also coordination number. The coordination number for the monocyclic ring is 2, whereas it

is 4 for the double ring. Among the closed structures studied, cage II is the most stable structure, due to the larger content of p character. In Fig. 8(d), we plot the minimum interatomic distances for various isomers. An increase in the interatomic distances in the double ring is seen over the monocyclic ring. This is due to increase in the coordination number in the double ring. The strains in the bonds also influence the interatomic distances. In cages I and III, due to larger bond strains, the boron atoms move away from each other, leading to a larger bond distance. As a result their binding energies are lowered.

The HOMO-LUMO gap shows a different behavior. In Fig. 8(b), we plot the HOMO-LUMO gap for these isomers, computed by the LDA and GGA. Unlike the binding energy, both methods give nearly same value for the gap, with the
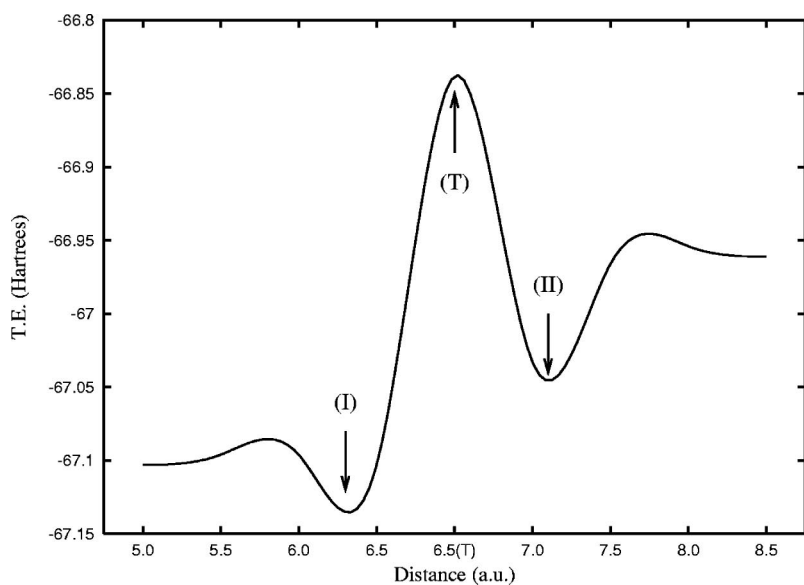
(a)
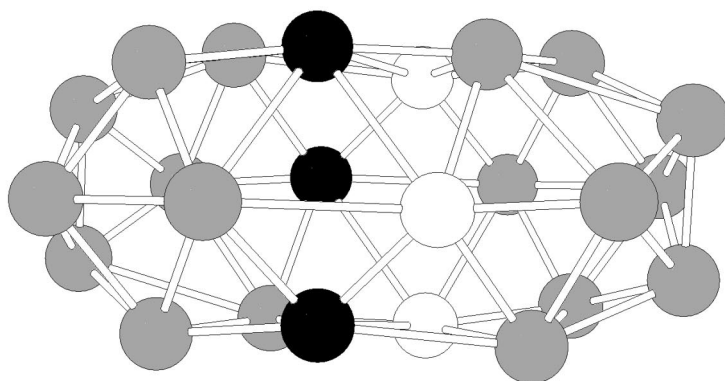
(b)

FIG. 9. (a) The total energy (in hartrees) of the clusters composed of two B_{12} icosahedra as they approach towards each other as a function of the intericosahedral distance. The arrows marked with (I) and (II) correspond to cages-I and II, respectively, while the arrow marked with (T) corresponds to the transition structure (cage-T) depicted in Fig. 9(b). (d) Cage T, the intermediate structure between cage I (Fig. 7[a(i)]) and cage II (Fig. 7[b(i)]), representing the transition state during the fusion of two icosahedra. It shows an intermediate stage of a formation of a completely relaxed staggered ring of six atoms (three white and three black).

exception of the double ring and isomer shown in Fig. 5(b), where the gap is lowered as expected, and cage III, where the gap is increased. The increase in the gap for cage III is due to the degenerate HOMO state. Moreover, a wide variation in the gap for various isomers is seen. The drum-shaped isomer [Fig. 4(a)], in spite of being nearly degenerate to the most stable structure, the double ring, exhibits a very small gap due to Jahn-Teller distortion. A similar behavior is also seen for cage III. The quasiplanar and convex isomers exhibit nearly the same HOMO-LUMO gap.

B. Fusion of two boron icosahedra

As mentioned earlier, a unit cell of α-rh boron hypothetical quasicrystal consists of a prolate unit cell and an oblate unit cell, stacked in a quasiperiodic manner. The prolate unit cell is slightly distorted which transforms into oblate unit cell. The mechanism of this transformation has been studied by Takeda *et al.*[15] and Boustani *et al.*[16]. Takeda *et al.* suggest that in order to undergo this transformation, the two icosahedra lying along the short body diagonal in the prolate unit cell should interpenetrate. Their model also suggests the removal of three interfacing atoms. On the other hand, Boustani *et al.* have shown that there is no need of removing any such atoms. Their investigation reveals that a much more stable closed tubular structure is formed upon fusion of the two icosahedra. To get a better insight into the fusion process, as the two icosahedra approach each other, we simulate the process by the following method. Two icosahedra were kept at various distances starting from 5.0 to 8.5 a.u., and a linear search for equivalent local minima was carried out. This distance is defined as the distance between the icosahedral centers. It is assumed that the composite B_{12}-B_{12} will take the structures corresponding to these local minima as they approach each other. Local geometry minimization was

carried out for nine different distances in the above-mentioned range. The corresponding total energies, in hartrees, of the equilibrium structures as a function of the distances are plotted in Fig. 9(a). This plot shows a barrier of 5.31 eV at a critical distance of 6.5 a.u., which the icosahedra have to cross in order to get fused. The composite structure of the two icosahedra sees a local minimum just before the barrier. The structure corresponding to this minimum is shown in Fig. 7[a(i)]. It can be seen that the icosahedra are bonded to each other by three bonds. Each black atom of the left icosahedra is bonded to the nearest white atom of the right icosahedra. As the icosahedra move further towards each other, these six atoms form a staggered ring like structure. Such staggering, as discussed earlier, facilitates sp^2 hybridization, thereby increasing the stability. At the barrier, an intermediate structure during the transition is seen. The geometry of this structure is depicted in Fig. 9(b). Due to the strained staggered ring, this structure is unstable. As the icosahedra move farther towards each other, the strains in the ring are reduced, finally giving a closed D_{3d} structure, shown in Fig. 7[b(i)]. A slight rearrangement is seen during the formation of this closed tubular structure. The atoms move towards the fusion region, consequently reducing the strains in the icosahedral units. This structure is the most stable cage isomer of B_{24} clusters. It is also nearly degenerate to the most stable isomer: i.e., the double ring. This structure (cage II) is about 1.91 eV lower than the structure corresponding to the local minima (cage I) just before the barrier. Thus, the effective barrier as seen by the fused structure is about 7.22 eV. As a result, the oblate unit cell becomes much more stable than the prolate unit cell. Hence, the transformation of the prolate unit cell to the oblate unit cell enhances the stability of the quasicrystal significantly.

IV. CONCLUSION

In the present work, we have reported the geometries and systematics of the bonding in various isomers of a 24-atom boron cluster and the fusion of two boron icosahedra using the BOMD method within the framework of density functional theory. We find that the monocyclic ring is the least stable structure. A staggered double-ring formation facilitates sp^2 hybridization, thereby making it the most stable structure. Our calculations reveal that a 24-atom boron cluster does form a closed 3D structures. The bonding analysis shows that a polarization of the bonds between the peripheral atoms is seen in the ring and planar isomers. The binding energy of all isomers is largely influenced by the amount of p character in the total charge density. An interesting observation common to all structures is the staggered arrangement of nearest-neighbor atoms. In the rings, the staggering is obtained by rotating the alternate rings, while in the open structures it is obtained by moving the atoms out of the plane as well as within the plane. Fusion occurs when the distance between the two icosahedra is less than a critical distance of about 6.5 a.u. In order to get fused, the icosahedra have to then cross a barrier of 5.31 eV. Such fusion enhances the stability of the quasicrystal significantly.

*Electronic mail: chacko@physics.unipune.ernet.in

†Electronic mail: kanhere@unipune.ernet.in

‡Electronic mail: boustani@uni-wuppertal.de

[1] H.W. Kroto *et al.*, Nature (London) **318**, 162 (1985).

[2] A.F. Hebard, M.J. Rosseinsky, R.C. Haddon, D.W. Murphy, S.H. Glarum, T.T.M. Palstra, A.P. Ramirez, and A.R. Kortan, Nature (London) **350**, 600 (1991); K. Holczer, O. Klein, S.M. Huang, R.B. Kaner, K.J. Fu, R.L. Whetten, and F. Diederich, Science **252**, 1154 (1991).

[3] *CRC Handbook of Chemistry and Physics*, edited by D. R. Lide (CRC Press, Boca Raton, 1995).

[4] Vijay Kumar and Yoshiyuki Kawazoe, Phys. Rev. Lett. **87**, 045503 (2001).

[5] E. L. Mutterties, *The Chemistry of Boron and its Compounds* (Wiley, New York, 1967); *Boron Hydride Chemistry*, edited by E. L. Mutterties (Academic, New York, 1975).

[6] S.J. La Placa, P.A. Roland, and J.J. Wynne, Chem. Phys. Lett. **190**, 163 (1992).

[7] S. Becker and H.J. Dietze, Int. J. Mass Spectrom. Ion Processes **73**, 157 (1986).

[8] L. Hanley, J.L. Whitten, and S.L. Anderson, J. Phys. Chem. **92**, 5803 (1988).

[9] J. Niu, B.K. Rao, and P. Jena, J. Chem. Phys. **107**, 132 (1997).

[10] I. Boustani, Phys. Rev. B **55**, 16 426 (1997).

[11] Wataru Hayami, Phys. Rev. B **60**, 1523 (1999).

[12] A. Katz and M. Duneau, J. Phys. (Paris) **47**, 181 (1986).

[13] D. Levine and P.J. Steinhardt, Phys. Rev. B **34**, 596 (1986).

[14] D. Levine and P.J. Steinhardt, Phys. Rev. Lett. **53**, 2477 (1984); D.S. Shechtman, I. Blech, D. Gratias, and J.W. Cahn, *ibid.* **53**, 1951 (1984).

[15] M. Takeda, M. Fujimori, A. Hori, and K. Kimura in *Proceedings of the 5th International Conference on Quasicrystals, Avignon, 1995*, edited by C. Janot and R. Mosseri (World Scientific, Singapore, 1995) p. 739.

[16] I. Boustani, A. Quandt, and P. Kramer, Europhys. Lett. **36**, 583 (1996).

[17] Ihsan Boustani, Angel Rubio, and Julio A. Alonso, Chem. Phys. Lett. **311**, 21 (1999); I. Boustani and A. Quandt, Europhys. Lett. **39**, 527 (1997); M.K. Sabra and I. Boustani, *ibid.* **42**, 611 (1998); Ihsan Boustani, Alexander Quandt, Eduardo Hernandez, and Angel Rubio, J. Chem. Phys. **110**, 3176 (1999); Ihsan Boustani, Chem. Phys. Lett. **233**, 273 (1995).

[18] M.C. Payne, M.P. Teter, D.C. Allan, T.A. Arias, and J.D. Joannopoulos, Rev. Mod. Phys. **64**, 1045 (1992).

[19] D. Vanderbilt, Phys. Rev. B **41**, 7892 (1990).

[20] D.M. Ceperley and B.J. Alder, Phys. Rev. Lett. **45**, 566 (1980).

[21] J.P. Perdew and Y. Wang, J. Chem. Phys. **45**, 13 244 (1992)

[22] G.B. Bachelet, D.R. Hamann, and M. Schlüter, Phys. Rev. B **26**, 4199 (1982).

[23] L. Kleinman and D.M. Bylander, Phys. Rev. Lett. **48**, 1425 (1982).

[24] B. Silvi and A. Savin, Nature (London) **371**, 683 (1994).

[25] W. L. Jorgensen and L. Salem, *The Organic Chemist's Book of Orbitals* (Academic, New York, 1973).

[26] Vienna *Ab initio* Simulation Package (VASP), Technishe Universität Wien, 1999.